

# Polarization-Induced pn Diodes in Wide-Band-Gap Nanowires with Ultraviolet Electroluminescence

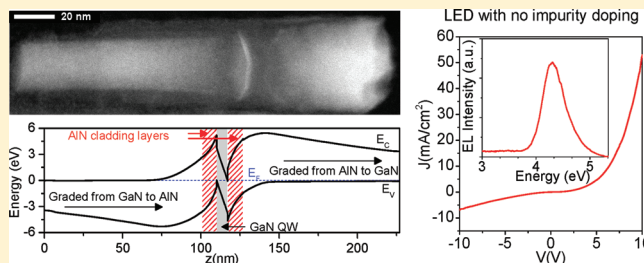
Santino D. Carnevale,<sup>†</sup> Thomas F. Kent,<sup>†</sup> Patrick J. Phillips,<sup>†</sup> Michael J. Mills,<sup>†</sup> Siddharth Rajan,<sup>†,‡</sup> and Roberto C. Myers<sup>\*,†,‡</sup>

<sup>†</sup>Department of Materials Science and Engineering and <sup>‡</sup>Department of Electrical and Computer Engineering, The Ohio State University, Columbus, Ohio 43210, United States

## Supporting Information

**ABSTRACT:** Almost all electronic devices utilize a pn junction formed by random doping of donor and acceptor impurity atoms. We developed a fundamentally new type of pn junction not formed by impurity-doping, but rather by grading the composition of a semiconductor nanowire resulting in alternating p and n conducting regions due to polarization charge. By linearly grading AlGa<sub>x</sub>N nanowires from 0% to 100% and back to 0% Al, we show the formation of a polarization-induced pn junction even in the absence of any impurity doping. Since electrons and holes are injected from AlN barriers into quantum disk active regions, graded nanowires allow deep ultraviolet LEDs across the AlGa<sub>x</sub>N band-gap range with electroluminescence observed from 3.4 to 5 eV. Polarization-induced p-type conductivity in nanowires is shown to be possible even without supplemental acceptor doping, demonstrating the advantage of polarization engineering in nanowires compared with planar films and providing a strategy for improving conductivity in wide-band-gap semiconductors. As polarization charge is uniform within each unit cell, polarization-induced conductivity without impurity doping provides a solution to the problem of conductivity uniformity in nanowires and nanoelectronics and opens a new field of polarization engineering in nanostructures that may be applied to other polar semiconductors.

**KEYWORDS:** Nanostructures, nitrides, molecular beam epitaxy, light-emitting diode, polarization, ultraviolet emission



In noncentrosymmetric crystal structures, for example wurtzite, spontaneous polarization can arise due to the ionic character of the bonds between atoms and their asymmetric positions within the structure. In essence, each unit cell of the material contains a dipole. In a bulk piece of such a material, the effects of this polarization are not normally manifest due to the dipoles in neighboring unit cells canceling out with each other. Therefore, the effects of polarization are more commonly seen at surfaces and interfaces (i.e., where the charge can no longer be canceled by neighboring unit cells). However, compositionally grading a thin film of a non-centrosymmetric crystal along the direction of the dipole can lead to n- or p-type conduction due to uniformly distributed bound polarization charge. The bound polarization charge arises because neighboring dipoles in the graded alloy are no longer of the same magnitude and therefore no longer completely cancel each other out. This raises or lowers the Fermi level with free charges being provided from surface states.<sup>1</sup> It was previously shown that electron<sup>2</sup> (n) or hole<sup>3</sup> (p) conduction could be produced in thin films of AlGa<sub>x</sub>N in which %Al is graded linearly. The polarization charge that occurs in III-nitrides is controllable by composition and strain engineering, and it provides numerous methods for modifying the band structure for electronic and optical devices.<sup>4</sup> Besides the uniform n- or p-type conducting regions<sup>2,3,5</sup> discussed above, high

electron density two-dimensional electron gases are formed due to polarization charge and utilized for high electron mobility transistors.<sup>6</sup> Also, the strong built-in electric field due to buried polarization charge allows for enhanced tunnel diodes<sup>7,8</sup> that could be used for multijunction solar cells or tunneling-induced multicolor light-emitting diodes (LEDs).<sup>9</sup> This study discusses polarization devices based in III-nitride nanowires. Nanowires increase the flexibility in polarization engineering since they accommodate strain better than epitaxial thin films,<sup>10</sup> allowing for the incorporation of the full compositional range of AlGa<sub>x</sub>N without suffering from strain-related defect formation. While III-nitride nanowires have been used to form LEDs for multicolor, solid-state lighting<sup>11–15</sup> and ultraviolet LEDs,<sup>15,16</sup> these devices are based on impurity-doped pn junctions. In this work, polarization engineering in III-nitrides is combined with compositional grading in nanowires to form a new type of pn junction not formed by impurity doping.

The design for a polarization-induced pn junction is shown in Figure 1. Grading Al<sub>x</sub>Ga<sub>1-x</sub>N (wurtzite crystal structure, Ga-face polarity) from  $x = 0$  to  $x = 1$  along the [0001] direction (Figure 1a) results in the Fermi level in the conduction band,

**Received:** November 11, 2011

**Revised:** December 14, 2011

**Published:** January 23, 2012

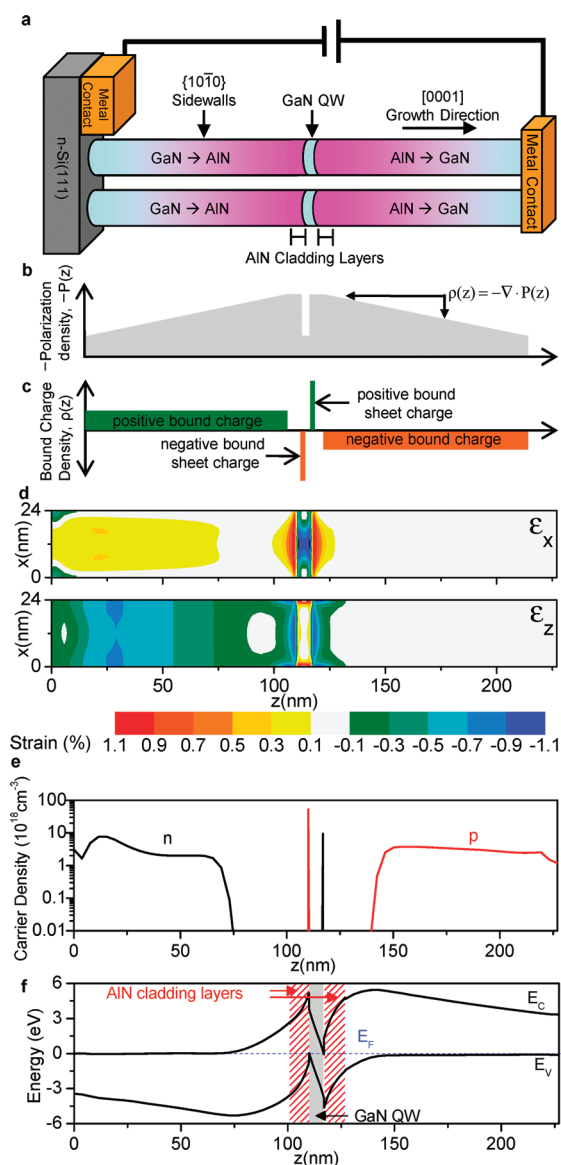


**Figure 1.** Polarization-induced pn junction formed in a semiconductor nanowire. (a) Schematic of device structure. (b) Polarization density as a function of nanowire length,  $z$ , and (c) positive and negative bound charge due to compositional grading. (d) Modeled strain profile in the  $x$  and  $z$  direction. (e) Modeled carrier density and (f) conduction and valence band edge energy along the length of the nanowire.

defining an n-type conducting region of the nanowire. An active region of a single 7 nm thick GaN quantum disk with 10 nm AlN cladding on either side of the well is grown. Next, a linearly graded AlGaIn section is grown in the reverse direction,  $x = 1$  to  $x = 0$  (Figure 1a), creating an opposite bound polarization charge (Figure 1c), which in turn results in a p-type conducting region. At the nanowire base, assuming the Anderson rule for determining band offsets and the approximate electron affinities,<sup>17</sup> a conduction band offset of 0.5–0.75 eV at the n-Si/n-GaN interface is expected, allowing for conduction from the n-type region of the nanowire into the n-Si wafer. A three-dimensional self-consistent strain and Poisson solver is used for modeling.<sup>18</sup> Because piezoelectric polarization can strongly alter the band diagram, strain is first modeled (Figure 1d). The strain values are used to compute the piezoelectric polarization,

and the composition is used to determine the spontaneous polarization charge. These values are then included in the Poisson solver to determine the carrier density profile (Figure 1e) and band diagram (Figure 1f). In this pn junction, the entire band gap offset between GaN and AlN (2.7 eV) is located in the valence band for the n-type region and in the conduction band for the p-type region. This large barrier prevents electrons and holes from overshooting the active region, thus providing built-in electron and hole blocking.

To realize this structure, we grow self-assembled, catalyst-free, GaN nanowires on n-Si (111) by plasma-assisted molecular beam epitaxy (PAMBE). The GaN nanowires are aligned perpendicular to the substrate and grow along the [0001] direction. Using a dynamic procedure,<sup>19</sup> nanowires are first nucleated at a lower temperature (720 °C), and then the substrate temperature is ramped to a higher temperature (780 °C), after which no new wires are nucleated, but existing wires continue to grow. The nanowire density is chosen to be  $\sim 400 \mu\text{m}^{-3}$ , resulting in an array of nearly identical nanowires (Figure 2a,b). This growth method provides exclusively vertical growth of GaN, while AlN continues to grow both vertically and coaxially resulting in the graded AlGaIn nanowires encased radially in wide-band-gap AlN. This coaxial layer seems to passivate the surface and prevent molecular charging effects (see Supporting Information). Compositional grading is accomplished by (anti)logarithmically ramping the temperature of Al and Ga effusion cells (see Supporting Information Figure 2) in order to linearly change the beam flux (Figure 2c). Composition is observed from Z-contrast scanning transmission electron microscopy (STEM) (Figure 2d) and energy-dispersive X-ray spectroscopy (EDXS) (Figure 2e), revealing the nanowires to be linearly graded as desired. However, the lengths of each layer of the device deviate from the target structure, likely due to a drop in vertical growth rate as nanowire diameter increases over time, consistent with AlN/GaN heterostructures we have previously grown.<sup>19</sup> The average length of the n-type and p-type regions are 110 and 60 nm, respectively. The length corrected band diagram (Figure 2f) still results in a pn junction. High-resolution X-ray diffraction and Z-contrast STEM measurements on other nanowires reveal that the grading is reproducible (see Supporting Information). Atomic resolution STEM micrographs do not exhibit visible defects like dislocations or inversion layers<sup>20</sup> (Figure 2g).

The diode behavior and optical emission from the polarization-induced nanowire LED (described above) are shown in Figure 3. The device contains additional Si impurity doping ( $1 \times 10^{19} \text{cm}^{-3}$ ) in the n-type graded region and Mg impurity doping ( $1 \times 10^{18}$ – $1 \times 10^{20} \text{cm}^{-3}$ ) in the p-type graded region. While pn junctions can be formed without any dopants, supplemental doping improves the conductivity in the n and p regions (see below and Supporting Information). At forward bias, current flows through the device leading to electron and hole injection and recombination in the quantum disk active region as indicated by the observation of rectification (Figure 3a, inset) and electroluminescence (EL) (Figure 3a–g). The emission energy strongly blue shifts from 2.4 eV at low bias to 3.29 eV at high bias (Figure 3b,c), typical for Ga-polar III-nitride LEDs due to the polarization charge at the AlN/GaN interfaces in the quantum disk, resulting in quantum confined Stark effect red shift of the EL. At small biases the peak emission energy is similar to the photoluminescence observed in nearly identical GaN/AlN quantum disk nanowires.<sup>21</sup> At high current densities ( $J$ ), the injected carriers screen the

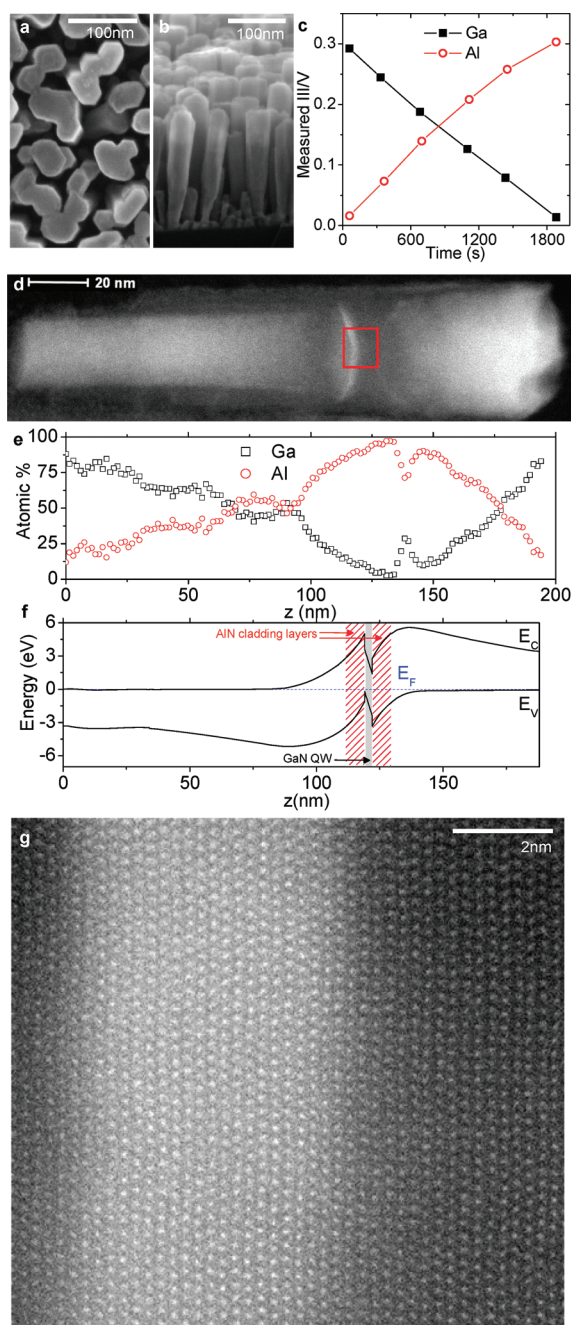


**Figure 2.** Growth and structure of compositionally graded nanowires. (a) Plan and (b) tilted scanning electron microscope (SEM) image view of graded AlGaIn nanowires on silicon wafers. (c) Beam flux of Ga and Al measured while logarithmically ramping the effusion cell temperature. Raw fluxes are converted to III/V based on the relation between Ga (Al) flux and the given supply of active nitrogen. (d) STEM image of a single nanowire heterostructure with Z-contrast to reveal GaN (lighter in the image) and AlN (darker). (e) EDXS measurement of Ga and Al composition as a function of position for a representative nanowire. (f) Modeled band diagram using the average nanowire dimensions obtained from STEM. (g) Atomic resolution STEM image of a GaN quantum disk (approximate location shown by red box in (d)) embedded in AlN within a representative nanowire.

polarization charge, reducing the Stark shift, leading to a strong blue shift. Emission close to the GaN band gap (3.4 eV) at high bias ( $V$ ) indicates full screening of the polarization charge in the quantum disks (Figure 3b,c).

To test whether the electrons and holes are provided by thermal ionization or by field ionization, the device is measured from room temperature to 15 K. Both normal  $J$ - $V$  and EL behavior persists to temperatures as low as 15 K (Figure 3e-g);  $J$  drops by  $\sim 20\%$  and EL intensity by  $\sim 80\%$  upon cooling. If hole conductivity were due to thermally ionized Mg-doping, the large ionization energy for holes in high %Al AlGaIn would lead to a several orders of magnitude increase in resistance at low temperature.<sup>3</sup> The large ionization energy of Mg in AlGaIn, determined by linearly interpolating the ionization energy of Mg in AlN (630 meV)<sup>22</sup> and GaN ( $\sim 200$  meV),<sup>3</sup> results in a negligible hole concentration at 15 K even with an Mg density of  $1 \times 10^{20}$  cm<sup>-3</sup>. Given that the devices shown here perform at cryogenic temperatures without an orders of magnitude drop in current or emission, the conclusion must be that Mg acceptors are not thermally ionized, but rather field-ionized. This proves the effectiveness of using compositionally graded nanowires for obtaining p-type (and n-type) Al<sub>x</sub>Ga<sub>1-x</sub>In with high Al compositions.

Additionally, the non-Arrhenius temperature dependence and conductivity at low temperatures indicates that electrons and holes likely tunnel from the n and p regions, respectively, directly into the active region. This is made possible by the polarization charge at the GaN/AlN interface, resulting in thin AlN tunnel barriers (Figure 3g, inset).  $J$  drops upon cooling from 300 to 140 K by  $\sim 20\%$ , perhaps due to thermally assisted tunneling. From 90 to 15 K,  $J$  increases by  $\sim 3\%$  perhaps due to reduced phonon scattering. Such an increase in conductivity at low temperature could not occur in AlGaIn if carriers are thermally ionized further evidence of field ionization leading to p-type conduction. No EL features indicative of carrier overshoot in the graded AlGaIn region are observed.

The EL of the polarization-induced LEDs can be pushed into the deep ultraviolet by using a wider-band-gap quantum disk active region (Figure 3h). This sample contains a 7 nm thick Al<sub>0.8</sub>Ga<sub>0.2</sub>In active region and displays clear rectification and band gap EL at 5 eV (Figure 3h). At low current densities and low temperatures, this device exhibits quantum disk emission (5 eV, black line); however, at higher current densities a broader EL peak at 4.2 eV is observed (red line) indicative of carrier overshoot and recombination in the graded AlGaIn regions (see Supporting Information). These results show the potential for using polarization-induced conduction in nanowires to create deep UV LEDs that might surpass planar devices. Deep UV planar devices currently exhibit low efficiency,<sup>23</sup> due in part to the highly resistive nature of high %Al p-AlGaIn.<sup>24</sup> This material is necessary because quantum wells made with wide-band-gap materials are needed to achieve LEDs that emit at low wavelengths. But confinement in wide-band-gap quantum wells requires an even wider-band-gap material to act as a barrier. Therefore, as researchers seek to push the emission of UV LEDs and lasers to shorter wavelengths, they will inevitably need to employ higher %Al AlGaIn. The device design put forth in this work seeks to avoid this problem by achieving superior p-AlGaIn conductivity using polarization-induced doping.<sup>3</sup> As a promising sign of this enhanced conductivity, nanowire samples in this study (see Supporting Information, Figure 5b) show better current densities at a given voltage when compared to some previously reported planar UV LEDs that emit at similar wavelengths.<sup>25</sup> Furthermore, since both the n- and p-type sides of the device are graded all the way to AlN, it should be possible to insert quantum wells into the active region with band gaps of very high %Al AlGaIn, theoretically allowing emission all the way down to the band

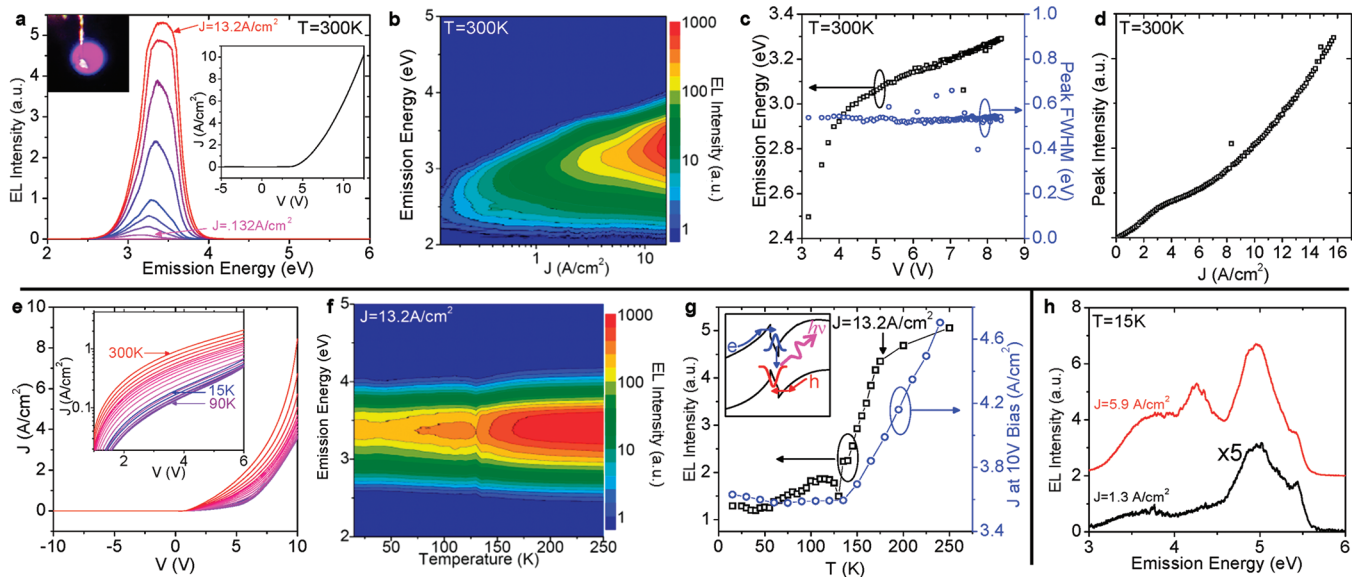


**Figure 3.** Diode behavior and ultraviolet light emission in polarization-induced pn junction nanowires. (a) EL spectra as a function of emission energy for the device described in Figures 1 and 2 plotted for various current densities ( $J$ ) (evenly spaced between the values indicated). (Left inset: photograph of device under forward bias. Right inset: linear scale  $J$  vs voltage ( $V$ ) measurements.) (b) EL intensity (color scale) as a function of emission energy and  $J$ . (c) Emission energy and FWHM as a function of  $V$ . (d) Peak intensity as a function of  $J$ . (e) Temperature ( $T$ ) variation of  $J$ - $V$  characteristics ( $T$  increases from 15 to 300 K by increments of 15 K). (Inset: same data shown in log scale.) (f) Emission intensity (color scale) as a function of emission energy and  $T$  for constant  $J$ . (g) Peak intensity at a constant  $J$  and  $J$  at a constant  $V$  as a function of  $T$ . (Inset: schematic showing tunneling in recombination process in active region.) (h) Low-temperature EL spectra at two different  $J$  for a sample with an active region consisting of  $\text{Al}_{0.8}\text{Ga}_{0.2}\text{N}$ .

gap of AlN (~200 nm). This illustrates a clear advantage of using nanowires instead of a planar geometry, since grading from GaN to AlN in thin films would strongly degrade the material quality due to misfit dislocations.

Until now, all of the experimental evidence shown has been for devices that take advantage of field-ionized Mg acceptors to achieve enhanced p-type conductivity in p-AlGaN. In addition to these devices, we have prepared, as a proof of principle, a polarization-induced pn junction containing no impurity doping (Figure 1) with a multiple quantum disk active region of three periods of 3 nm thick  $\text{Al}_{0.8}\text{Ga}_{0.2}\text{N}$  with 5 nm thick AlN barriers. The  $J$ - $V$  curves reveal rectifying behavior with a turn-on voltage near 3 V (Figure 4a, red line). EL spectra from this impurity doping free pn junction reveal an ultraviolet peak at 4.4 eV (Figure 4b, red curve), showing that electrons and holes radiatively recombine. These results demonstrate a new semiconductor diode formed without any impurity doping.

Importantly, previous work showed that polarization-induced hole conductivity is only possible in planar AlGaN if the film is doped with Mg,<sup>3</sup> whereas in graded nanowires shown here, Mg doping is not needed. One explanation is that the large surface-to-volume ratio of the nanowires leads to a larger number of surface acceptors than background donors. For polarization-induced p-type doping, surface acceptors from the exposed m-plane of the nanowires will be ionized. A simple calculation shows that for an unintentionally doped nanowire the ratio of acceptor states to donor states is given by

$$\frac{N_A}{N_D} = \frac{\sigma_A^{\text{surf}} \times 2\pi rh}{\rho_D^{\text{back}} \times \pi r^2 h} = \frac{2\sigma_A^{\text{surf}}}{\rho_D^{\text{back}} r}$$

where  $N_A$  is the total number of acceptor states,  $N_D$  is the number of donor states,  $\sigma_A^{\text{surf}}$  is the density of acceptor-like surface states,  $\rho_D^{\text{back}}$  is the density of donor states due to

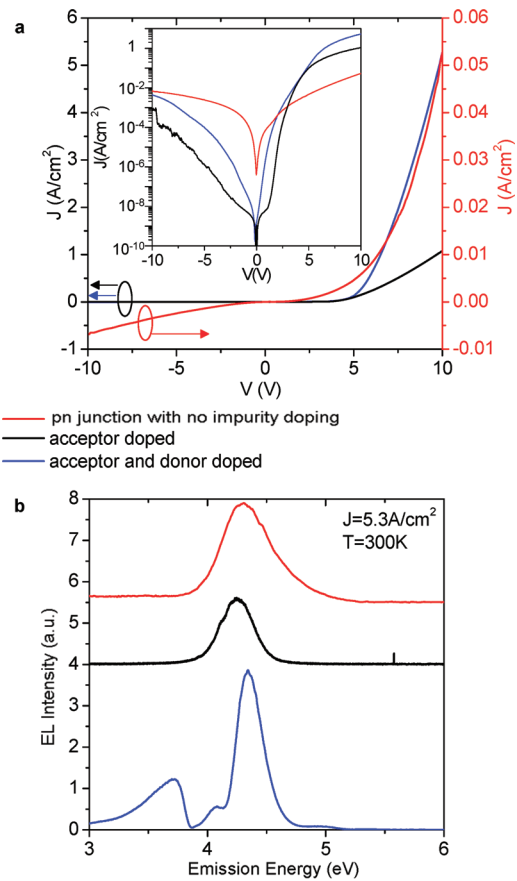


**Figure 4.** No impurity doping pn junction and effect of supplemental doping. (a) Linear  $J$ - $V$  characteristics and (b) EL spectra for polarization-induced pn junction nanowires with or without supplemental impurity doping as indicated in the figure.

unintentional background doping,  $r$  is the nanowire radius, and  $h$  is its height. Putting in typical values for the constants on the right side of the equation ( $\rho_{\text{D}}^{\text{back}} = 10^{17} \text{ cm}^{-3}$  (ref 26),  $\sigma_{\text{A}}^{\text{surf}} = 10^{12} \text{ cm}^{-2}$  (ref 27),  $r = 20 \text{ nm}$ ) shows that for every donor state there are 10 acceptor states. However, as radius increases, this ratio of acceptors to donors will obviously decrease, making it more and more difficult to achieve p-type material. It is therefore imperative to keep  $r$  as small as possible if polarization-induced p-type material is to be achieved without Mg doping.

A similar expression to the one above applies to planar films, for which the ratio of acceptor states to donor states will be inversely proportional to the film's thickness ( $t$ ). Polarization-induced hole conductivity in thin films without Mg requires compositionally grading thin films over the full AlGaIn compositional range within a small thickness (for  $N_{\text{A}}/N_{\text{D}} = 10$ , then  $t = 10 \text{ nm}$ ); thus, the appropriate planar structure might be prohibitively difficult to synthesize in light of strain-induced defect formation. In the nanowires presented in this study, composition is graded in the vertical direction with little change in the radius of the wire. This makes it possible to compositionally grade the p-type region over an arbitrary length of nanowire without decreasing the surface-to-volume ratio or the ratio of acceptor states to donor states.

As previously discussed, the conductivity of the nanowires can be further increased by supplementing the polarization-induced electrons or holes with impurity doping. We compare three types of polarization-induced pn junctions: impurity doping free, acceptor doped (Mg), and acceptor (Mg) and donor (Si) doped (Figure 4). Supplementing the polarization-induced p-type region with acceptors leads to a factor of 20 increase in current at a given bias, and including both acceptors and donors increases the current by another factor of 5 (Figure 4a). Both the impurity doping free and doped nanowires exhibit EL with similar intensity for lower current densities (Figure 4b). Impurity doping introduces additional below band gap EL perhaps due to impurity-related recombination. In the current nanowire design, conductivity is greatly improved by supplemental doping of impurities, which are field-ionized. As could be expected, p-type conductivity is more strongly improved by supplemental doping, whereas supplemental Si doping has a smaller effect. This observation is further supported by  $I$ - $V$  measurements of polarization-induced n-type nanowires shown in Supporting Information Figure 3 (graded from  $x = 0$  to  $x = 1$  only). Supplemental Si-doping results in only a small increase in  $dI/dV$  compared with impurity doping free n-type nanowires. Surprisingly,  $dI/dV$  of the impurity doping free polarization-induced AlGaIn nanowires is better than  $dI/dV$  of Si-doped GaN nanowires, whereas 50% Al average composition n-AlGaIn should be expected to exhibit a much smaller conductivity than n-GaN. Again, this demonstrates a clear advantage of polarization engineering in nanowires for improved n- and p-type conductivity in AlGaIn.

Future work will focus on improving the performance of the impurity doping free devices, described above. Given that this is the first device of its kind, there are many possible strategies for improving conductivity in the impurity doping free devices, for example, grading composition over shorter lengths to increase the bound polarization charge or using nanowires with smaller radii and reducing background donor levels to boost  $N_{\text{A}}/N_{\text{D}}$ . One particularly interesting possibility is to functionalize the nanowire surface. This would not only allow for a better understanding of how surface states impact polarization-induced doping, but by adjusting the surface states

on the nanowire sidewalls, it should also allow for modulation of the carrier concentrations in the device. In fact, in our initial nanowire devices that were not AlN passivated, EL was only observed when the samples were exposed to air and disappeared in vacuum accompanied by a more than 4 V bias drop at constant current (see Supporting Information Figure 1), suggesting that molecular charging at the nanowire surfaces strongly affect conductivity and recombination processes. With increased carrier concentrations, impurity doping free devices might rival those that employ traditional impurity doping by avoiding the deleterious impacts, such as additional recombination sites and changes in carrier lifetimes, associated with adding impurities to a material. Impurity doping free devices may also prove important for nanoscale devices because they will allow for uniform doping profiles within a nanostructure not possible with random impurity doping.

Our results demonstrate a new type of pn junction not formed by impurity doping. Polarization engineering in III-nitride nanowires provides a robust and reproducible method for electron and hole conductivity in wide-band-gap semiconductors. In total, 16 different polarization-induced pn junction nanowire LED samples were prepared, and all samples revealed clear diode behavior and ultraviolet light emission (see Supporting Information). Because electrons and holes are injected from AlN barriers ( $E_{\text{g}} = 6.2 \text{ eV}$ ), LEDs spanning the full band gap range of AlGaIn (3.4–6.2 eV) are possible. We observed EL at various wavelengths from 250 nm in  $\text{Al}_{0.8}\text{Ga}_{0.2}\text{N}$  quantum disk LEDs to 360 nm in GaN quantum disk LEDs. The conductivity and EL show slight variation with temperature, verifying that the electrons and holes are polarization-induced (field-ionized), rather than thermally ionized from impurities. Since polarization charge is built into the unit cell, the nanowire doping profile (in the devices without impurity doping) is uniform unlike randomly impurity-doped wires. Polarization engineering in nanowires allows the band engineer to make full use of the range of band gap and polarization in AlGaIn and InGaIn alloys. Similar devices might also be possible in other polar semiconductor systems, such as ZnMgO or  $\text{LiNbO}_3$ . We can envision using polarization-induced pn junctions in new types of transistors, photodetectors, solar cells, or lasers using polar semiconductor nanowires.

## ■ ASSOCIATED CONTENT

### 📄 Supporting Information

Discussion of growth and characterization methods, surface passivation effects of two-step growth, polarization-doped n-type nanowires, carrier overshoot, and a list of all samples grown for this study. This material is available free of charge via the Internet at <http://pubs.acs.org>.

## ■ AUTHOR INFORMATION

### Corresponding Author

\*E-mail: [myers.1079@osu.edu](mailto:myers.1079@osu.edu).

## ■ ACKNOWLEDGMENTS

We acknowledge Mark O'Steen (VEECO) for supplying the initial recipe for compositional MBE grading. This work was supported by the Office of Naval Research (N00014-09-1-1153) and by the National Science Foundation CAREER award (DMR-1055164). S.D.C. acknowledges support from the National Science Foundation Graduate Research Fellowship Program (2011101708).

## ■ REFERENCES

- (1) Ibbetson, J.; Fini, P.; Ness, K.; DenBaars, S.; Speck, J.; Mishra, U. Polarization effects, surface states, and the source of electrons in AlGa<sub>x</sub>N/GaN heterostructure field effect transistors. *Appl. Phys. Lett.* **2000**, *77*, 250–252.
- (2) Jena, D.; Heikman, S.; Green, D.; Buttari, D.; Coffie, R.; Xing, H.; Keller, S.; DenBaars, S.; Speck, J. S.; Mishra, U. K.; Smorchkova, I. Realization of wide electron slabs by polarization bulk doping in graded III-V nitride semiconductor alloys. *Appl. Phys. Lett.* **2002**, *81*, 4395–4397.
- (3) Simon, J.; Protasenko, V.; Lian, C.; Xing, H.; Jena, D. Polarization-induced hole doping in wide-band-gap uniaxial semiconductor heterostructures. *Science* **2010**, *327*, 60–64.
- (4) Jena, D.; Simon, J.; Wang, A.; Cao, Y.; Goodman, K.; Verma, J.; Ganguly, S.; Li, G.; Karda, K.; Protasenko, V.; Lian, C.; Kosel, T.; Fay, P.; Xing, H. Polarization-engineering in group III-nitride heterostructures: New opportunities for device design. *Phys. Status Solidi A* **2011**, *208*, 1511–1516.
- (5) Rajan, S.; Xing, H. L.; DenBaars, S.; Mishra, U. K.; Jena, D. AlGa<sub>x</sub>N/GaN polarization-doped field-effect transistor for microwave power applications. *Appl. Phys. Lett.* **2004**, *84*, 1591–1593.
- (6) Khan, M.; Bhattarai, A.; Kuznia, J.; Olson, D. High-electron-mobility transistor based on a GaN-Al<sub>x</sub>Ga<sub>1-x</sub>N Heterojunction. *Appl. Phys. Lett.* **1993**, *63*, 1214–1215.
- (7) Grundmann, M. Thesis. Polarization-induced tunnel junctions in III-nitrides for optoelectronic applications, University of California, Santa Barbara, 2007.
- (8) Krishnamoorthy, S.; Nath, D. N.; Akyol, F.; Park, P. S.; Esposto, M.; Rajan, S. Polarization-engineered GaN/InGa<sub>x</sub>N/GaN tunnel diodes. *Appl. Phys. Lett.* **2010**, *97*, 203502.
- (9) Grundmann, M. J.; Mishra, U. K. Multi-color light emitting diode using polarization-induced tunnel junctions. *Phys. Status Solidi C* **2007**, *4*, 2830–2833.
- (10) Thillosen, N.; Sebald, K.; Hardtdegen, H.; Meijers, R.; Calarco, R.; Montanari, S.; Kaluza, N.; Gutowski, J.; Luth, H. The state of strain in single GaN nanocolumns as derived from micro-photoluminescence measurements. *Nano Lett.* **2006**, *6*, 704–708.
- (11) Qian, F.; Gradecak, S.; Li, Y.; Wen, C. Y.; Lieber, C. M. Core/multishell nanowire heterostructures as multicolor, high-efficiency light-emitting diodes. *Nano Lett.* **2005**, *5*, 2287–2291.
- (12) Hong, Y. J.; Lee, C.; Yoon, A.; Kim, M.; Seong, H.; Chung, H. J.; Sone, C.; Park, Y. J.; Yi, G. Visible-color-tunable light-emitting diodes. *Adv. Mater.* **2011**, *23*, 3284.
- (13) Armitage, R.; Tsubaki, K. Multicolour luminescence from InGa<sub>x</sub>N quantum wells grown over GaN nanowire arrays by molecular-beam epitaxy. *Nanotechnology* **2010**, *21*, 195202.
- (14) Guo, W.; Zhang, M.; Banerjee, A.; Bhattacharya, P. Catalyst-free InGa<sub>x</sub>N/GaN nanowire light emitting diodes grown on (001) silicon by molecular beam epitaxy. *Nano Lett.* **2010**, *10*, 3355–3359.
- (15) Lee, S.; Kim, T.; Lee, S.; Choi, K.; Yang, P. High-brightness gallium nitride nanowire UV-blue light emitting diodes. *Philos. Mag.* **2007**, *87*, 2105–2115.
- (16) Motayed, A.; Davydov, A. V.; He, M.; Mohammad, S. N.; Melngailis, J. 365 nm operation of n-nanowire/p-gallium nitride homojunction light emitting diodes RID F-7773-2010. *Appl. Phys. Lett.* **2007**, *90*, 183120.
- (17) Adachi, S. *Handbook on Physical Properties of Semiconductors*; Kluwer Academic Publishers: Dordrecht, 2004; Vols. 1–3.
- (18) <http://www.nextnano.de/nextnano3/>.
- (19) Carnevale, S. D.; Yang, J.; Phillips, P. J.; Mills, M. J.; Myers, R. C. Three-dimensional GaN/AlN nanowire heterostructures by separating nucleation and growth processes. *Nano Lett.* **2011**, *11*, 866–871.
- (20) Ristic, J.; Calleja, E.; Sanchez-Garcia, M.; Ulloa, J.; Sanchez-Paramo, J.; Calleja, J.; Jahn, U.; Trampert, A.; Ploog, K. Characterization of GaN quantum discs embedded in Al<sub>x</sub>Ga<sub>1-x</sub>N nanocolumns grown by molecular beam epitaxy. *Phys. Rev. B* **2003**, *68*, 125305.
- (21) Renard, J.; Songmuang, R.; Tourbot, G.; Bougerol, C.; Daudin, B.; Gayral, B. Evidence for quantum-confined Stark effect in GaN/AlN quantum dots in nanowires. *Phys. Rev. B* **2009**, *80*, 121305.
- (22) Taniyasu, Y.; Kasu, M.; Makimoto, T. An aluminium nitride light-emitting diode with a wavelength of 210 nanometres. *Nature* **2006**, *441*, 325–328.
- (23) Kneissl, M.; Kolbe, T.; Chua, C.; Kueller, V.; Lobo, N.; Stellmach, J.; Knauer, A.; Rodriguez, H.; Einfeldt, S.; Yang, Z.; Johnson, N. M.; Weyers, M. Advances in group III-nitride-based deep UV light-emitting diode technology. *Semicond. Sci. Technol.* **2011**, *26*, 014036.
- (24) Khan, A.; Balakrishnan, K.; Katona, T. Ultraviolet light-emitting diodes based on group three nitrides. *Nature Photonics* **2008**, *2*, 77–84.
- (25) Adivarahan, V.; Wu, S.; Zhang, J.; Chitnis, A.; Shatalov, M.; Mandavilli, V.; Gaska, R.; Khan, M. High-efficiency 269 nm emission deep ultraviolet light-emitting diodes. *Appl. Phys. Lett.* **2004**, *84*, 4762–4764.
- (26) Stoica, T.; Calarco, R. Doping of III-Nitride Nanowires Grown by Molecular Beam Epitaxy. *IEEE J. Sel. Top. Quantum Electron.* **2011**, *17*, 859–868.
- (27) Chevtchenko, S.; Ni, X.; Fan, Q.; Baski, A.; Morkoc, H. Surface band bending of a-plane GaN studied by scanning Kelvin probe microscopy RID A-1635-2011. *Appl. Phys. Lett.* **2006**, *88*, 122104.